

# PARAMETER IDENTIFICATION OF A RIGID-FLEXIBLE SATELLITE USING KALMAN FILTER

## Adriana Trigolo

INPE - Instituto Nacional de Pesquisas Espaciais  
CP 515 - São José dos Campos, SP  
CEP 12227-010  
E-mail: trigolo@dem.inpe.br

## Hélio Koiti Kuga

INPE - Instituto Nacional de Pesquisas Espaciais  
CP 515 - São José dos Campos, SP  
CEP 12227-010  
E-mail: hkk@dem.inpe.br

## Luiz Carlos Gadelha de Souza

INPE - Instituto Nacional de Pesquisas Espaciais  
CP 515 - São José dos Campos, SP  
CEP 12227-010  
E-mail: gadelha@dem.inpe.br

**Abstract.** Nowadays an increasing number of space missions are using satellites whose structure consists basically of two parts. The first one is the body of the satellite, which contains all instrumentation involved with the objectives of the mission, including the Attitude Control Systems (ACS). That structure must be rigid enough to support the mechanical load during the launch phase and along the mission. The second one, consists of long and/or wide flexible appendices, such as solar panels, communication antennas, telescopic structures, robotics flexible arms, whose purpose are to get solar energy, to manipulate equipment or to place some sensors out of interference range of the satellite main body. The satellite structure must be as light as possible in order to save fuel in the launch phase and to allow its manufacturing. These both requirements impose a commitment between rigidity and flexibility. The increasing need for better pointing accuracy of antennas connected to the rigid part of the spacecraft leads to a requirement for more efficient controllers, which in turn calls for more accurate identification process. To meet the requirements for pointing accuracy, flexible parameters as elastic displacement, which are of great importance for control tasks should be continuously identified in the space environment. This paper presents the results from a study of elastic displacement identification using the Kalman Filter methodology. A flexible Euler-Bernoulli beam, connected to a rigid core with torques as input and angles and angular velocities as outputs is used as simple mathematical model of a rigid-flexible satellite to apply the Kalman filter identification algorithm proposed. The Kalman filter is tested under several conditions considering cold start with coarse initial knowledge and varied measurement noise levels. At the end comments are drawn about the robustness of the proposed procedure and feasibility of implementation within the control system loop.

**Keywords.** Flexibility, Dynamics, Parameter Identification, and Kalman Filter

## 1. Introduction

The use of small satellites has been a fast, simple and of low cost way of reaching the space in missions with the most several applications (Guerra, 1997; Souza, 1999), however, in order to conquer the space it is necessary to launch spacecraft that involves rigid/flexible structures. These missions are more complex because the satellites have a great number of components like, solar panels, antennas, cameras and/or mechanical manipulators. As a results, the influence of the flexibility of such structure play a important role in the dynamics behavior as well as in the performance of the Attitude Control System (ACS) Silva et al (1998). Others important aspects in the study of the dynamics and control of flexible space structures are: the degree of interaction between the rigid and flexible motion, maintenance of the ACS performance in face the uncertainties of the mathematical model, damping residual vibrations in order to keep pointing precision and dynamic parameters identification Silva et al (2002). This paper presents an identification procedure using the Kalman Filter methodology that may be used to identify the elastic displacement and/or system parameters in space. Section 2 presents a mathematical model of a simple spacecraft based on a flexible Euler-Bernoulli beam connected to a rigid core. The equations of motion are also derived where the torque is used as input and angles and angular velocities as outputs. Section 3 presents the Kalman filter identification algorithm. Section 4 presents the simulation where the Kalman filter is tested under several conditions considering cold start with coarse initial knowledge and varied measurement noise levels. Section 5 concludes the paper.

## 2. Spacecraft Mathematical Model

The satellite mathematical model used is composed of a rigid platform with two flexible appendixes and masses in the extremities of the appendixes. The appendixes are identical and opposite, being considered as beam connected to the platform, and subjects to rotational and vibrational motion. In order to derive the equations of motion for this model, one applies the Lagrange methodology, starting from the expression of the kinetics and potential energy of the system. Fig. 1 illustrates the system composed by rigid hub, an elastic appendage with a mass in the extremity.

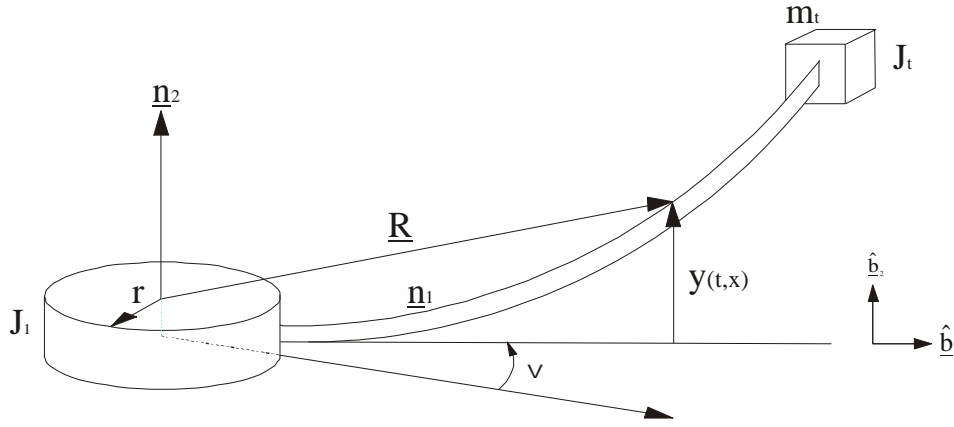


Figure 1. Satellite model composed by a rigid hub, an elastic appendage with a mass in the extremity.

One considers that the inertial reference system, coincides with the origin of the fixed reference system in the rigid body and it is represented by the axes  $n_1, n_2, n_3$ . The fixed reference system in the rigid body, coincides with the center of mass of the rigid body, which is characterized by the axes  $b_1, b_2, b_3$ . The vector  $r$  represents the radius of the rigid body. The vector  $x$  represents a position of a measured mass element along the appendage in the no deformed form, in relation to the appendage reference system. The vector position of any point in the appendage relative to the inertial reference system is given by  $R$ . The vector of elastic displacement (elastic deformation) measured perpendicular to the axis  $b_1$  is represented by  $y(x, t)$ . Therefore, the vector position of any point in the deformed appendage form, relative to the inertial reference system is given for:

$$\underline{R}_1 = (r+x) \hat{b}_1 + y \hat{b}_2 \quad (1)$$

and its velocity vector is

$$\underline{R} = \frac{d}{dt}(\underline{R})_N = \frac{d}{dt}(\underline{R})_B + \underline{\omega} \times \underline{R} \quad (2)$$

considering that  $\dot{\theta}$  is the satellite angular velocity and substituting Eq. (1) into (2), one has

$$\underline{\dot{R}} = -\dot{\theta} y \hat{b}_1 + [\dot{\theta}(r+x) + \dot{y}] \hat{b}_2 \quad (3)$$

## 2.1. Equation of Motion

The total kinetics energy of the system is given by

$$T_{\text{Total}} = T_{\text{disk}} + T_{\text{app}} + T_{\text{tip}} \quad (4)$$

$$T = \frac{1}{2} J_1 \dot{\theta} + \dot{\theta} \left[ \int_0^L \rho (r+x)^2 dx + m_t (r+x)^2 + J_t \right] + \int_0^L \rho \dot{y}^2 dx + m_t \{ \dot{y}(L)^2 \} + J_t \{ \dot{y}'(L) \}^2 + 2\dot{\theta} \left\{ \int_0^L \rho \dot{y} (r+x) dx + m_t (r+L) \dot{y}(L) + J_t \dot{y}'(L) \right\} \quad (5)$$

where  $J_1$  is the rigid body moment of inertia of the,  $\rho$  is the density of mass of the appendage, and  $L$  is the length of the appendage,  $m_t$  and  $J_t$  are the mass and moment of inertia of the mass at the end of the appendage and  $y(x, t)$  represents the elastic displacement.

The total potential energy  $V$  is considered as entirely due to the elastic deformations of the system and it is given by

$$V_T = \frac{1}{2} \int_0^L (EI) \left( \frac{\partial^2 y}{\partial x^2} \right)^2 dx + \frac{1}{2} \int_0^L (EI) \left( \frac{\partial^2 y}{\partial x^2} \right)^2 dx = \int_0^L (EI) \left( \frac{\partial^2 y}{\partial x^2} \right)^2 dx \quad (6)$$

where E represents the module of elasticity (module of Young) and I the moment of inertia of the beam. The discretization of the system is done using assumed mode method (Trigolo, 2002). Therefore, the elastic displacement  $y(x,t)$  is substituted by

$$y(x,t) = \sum_1^N \phi_j(x) q_{ji}(t) \quad (7)$$

where  $\phi_j(x)$  are the admitted functions and  $q_{ji}(t)$  are the generalized coordinates. The equations of motion are found for the rotation  $\theta(t)$  and elastic  $q(t)$  motion, using the Lagrange formulation

$$\frac{d}{dt} \left( \frac{\partial T}{\partial \dot{x}_i} \right) - \frac{\partial T}{\partial x_i} + \frac{\partial V}{\partial x_i} = F_{x_i}, \quad (i=1,2) \quad (8)$$

Substituting the kinetic and potential energy expression into Eq.(8) and after some manipulation the equations of motion are given by

$$J_1 \ddot{\theta} + 2\ddot{\theta} \left[ \int_0^L \rho(r+x)^2 dx + m_t (r+L)^2 + J_t \right] + 2 \left[ \int_0^L \rho(r+x) \phi_i(x) dx + m_t (r+L) \phi_i(L) + J_t \phi_i'(L) \right] \ddot{q} = u \quad (9)$$

and

$$2 \ddot{\theta} \left\{ \int_0^L \rho(r+x) \phi_i(x) dx + m_t (r+L) \phi_i(L) + J_t \phi_i'(L) \right\} + 2 \left\{ \int_0^L \rho \phi_j(x) \phi_i(x) dx + m_t \phi_j(L) \phi_i(L) + J_t \phi_j'(L) \phi_i'(L) \right\} \ddot{q} + 2 \int_0^L (EI) \phi_j''(x) \phi_i''(x) q dx = 0 \quad (10)$$

The equations of motion in the matrix form is

$$\begin{bmatrix} \hat{J} & M_{\theta q}^T \\ M_{\theta q} & M_{qq} \end{bmatrix} \cdot \begin{bmatrix} \ddot{\theta} \\ \ddot{q} \end{bmatrix} + \begin{bmatrix} 0 & 0 \\ 0 & K_{qq} \end{bmatrix} \cdot \begin{bmatrix} \theta \\ q \end{bmatrix} = \begin{bmatrix} 1 & 0 \\ 0 & 0 \end{bmatrix} \cdot \begin{bmatrix} u \\ 0 \end{bmatrix} \quad (11)$$

where  $\hat{J}$  is the total inertia moment of the system,  $M_{\theta q}$  represents the sub-matrix associated with the rigid and flexible motion,  $M_{qq}$  represents the sub-matrix associated with the flexible motion and  $K_{qq}$  represents the sub-matrix associated with flexible body. The matrix form in compact form is given by

$$M \ddot{x} + K x = D u \quad (12)$$

where M is the mass matrix, K is the stiffness matrix of the system and D is the control influence matrix (Trigolo, 2002). Eq.(12) in state space modal form is given by

$$\tilde{M} \ddot{\eta}(t) + \tilde{C} \dot{\eta}(t) + \tilde{K} \eta(t) = \tilde{D} u \quad (13)$$

where  $\tilde{M}$ ,  $\tilde{C}$ ,  $\tilde{K}$  and  $\tilde{D}$  represents mass, damping, stiffness and control influence matrices in modal form.

### 3. Kalman Filter Identification Algorithm

The Kalman filter is a computational algorithm containing a sequence of time and measurement updatings of the estimates of the system state Gelb et al (1974). The Kalman filter can incorporate dynamic noise in the dynamical model of the state. It is a real time estimator supplying the estimates for the instant that the measurement is available. The filter consists of two cycles:

- Time update
- Measurement update

In synthesis the Kalman filter processes measurements to produce an estimate of minimum variance of the state of a system using the knowledge of the dynamics of the system, and of the measurement, the statistics of the noise of the dynamic system, and errors of the measurements, besides the information of the initial condition (Chiaradia, 2002).

### 3. 1. State Dynamics Model

Let state dynamical model be represented by:

$$\dot{x} = A x + G \omega \quad (14)$$

where  $x = (\theta, \dot{\theta}, \ddot{\theta}, \dot{\ddot{\theta}})$  is the state continuously variant in the time,  $G$  is a matrix of addition of dynamic noise,  $w$  is the continuous dynamic noise and  $A$  is named the system matrix that relates the state timely and linearly, given by:

$$A = \begin{bmatrix} 0 & | & I \\ \hline -\tilde{K} & | & -\tilde{C} \end{bmatrix} \quad (15)$$

The system matrix is formed by the identity matrix  $I$ , by  $\tilde{K} = \text{diag}\{0, \omega_2^2\}$  the matrix containing the squared natural frequencies, and the modal damping matrix  $\tilde{C} = \{0, 2\xi_2 \omega_2\}$ .

### 3. 2. Measurements Model

The measurement model is given by:

$$y = H x + v \quad (16)$$

where  $y$  is the measurement vector composed by the angle  $(\theta)$  and angular velocity  $(\dot{\theta})$  observables. The measurements  $\theta$  and  $\dot{\theta}$  are collected by a position and velocity sensor. For the angular position and velocity it was assumed nominally a standard deviation of  $0.1^0$  and  $0.01^0/s$ , respectively. The  $H$  matrix relates the measurements to the state by:

$$H = \begin{bmatrix} 1 & 0 & 0 & 0 \\ 0 & 0 & 1 & 0 \end{bmatrix} \quad (17)$$

and  $v$  represents a white noise vector to model the errors during the measurement process, with the following statistical characteristics

$$v_{\theta} = N(0, 0.1^0) \quad \text{and} \quad v_{\dot{\theta}} = (0, 0.01^0 / s) \quad (18)$$

### 3. 3. Time update

In this filter cycle, the state and covariance estimates are computed by using the dynamical model of the system. The time updated state  $\bar{x}$ , and covariance  $\bar{P}$  are computed by:

$$\dot{\bar{x}} = A \bar{x} \quad (19)$$

with initial condition  $\bar{x}_{k-1} = \hat{x}_{k-1}$ , and

$$\dot{\bar{P}} = A \bar{P} + \bar{P} A^t + G Q G^t \quad (20)$$

with initial condition  $\bar{P}_{k-1} = \hat{P}_{k-1}$ . Equation (20) is known as the continuous Riccati equation. In this work, Eq. (19) and (20) are solved numerically using the Runge-Kutta method embedded in the Matlab package.

### 3. 4. Measurement update

This cycle updates the state and covariance matrix at instante k due to measurements  $y_k$ , by means of the measurement model given by Equation (16). The measurements of instante k provide the information to update the state and covariance. The equations that follow describe the measurement update cycle of Kalman filter:

$$K = \bar{P} H^t (H \bar{P} H^t + R)^{-1} \quad (21)$$

$$\hat{P} = (I - KH) \bar{P} \quad (22)$$

$$\hat{x} = \bar{x} + K (y - H \bar{x}) \quad (23)$$

where K represents the Kalman gain, and  $\hat{P}$  and  $\hat{x}$  are the covariance and the state updated. The errors between the actual state and the estimated state will be used to evaluate the algorithm performance for the tests carried out. The errors were defined by:

$$\text{Estimated error standard deviation} \quad \Delta \hat{\epsilon}_i = P_{ii}^{1/2} \quad (24)$$

$$\text{Actual error} \quad \Delta \epsilon_i = x_i - \hat{x}_i \quad (25)$$

## 4. Simulations

The aim of the simulations is to implement and test a Kalman filter for identification of the flexible mode (elastic displacement) of a rigid flexible satellite. The analysis is performed through the utilization of the dynamical model equation (14) and Equations (16) to (23), which represent the time and measurement update of the state and covariance via the Kalman filter. The simulations were carried out by computational implementation of the software in Matlab language. First of all, an analysis for the nominal case is made using the initial conditions and parameters shown in Table 1. Next, the same conditions used in the nominal case are applied to analyze the behavior of the filter when non-typical measurement errors are imposed on purpose. Two cases comprising precise and imprecise measurements are shown and compared to the nominal case.

Table 1. Initial conditions and tuned parameters of the Kalman filter

Symbol	Initial Values	Symbol	Initial Values	Symbol	Initial Values
G	$I_4$	$P_{\dot{\theta}}$ ( $^0/s$ ) <sup>2</sup>	$(10)^2$	$Q_{\dot{\theta}}$ ( $^0/s$ ) <sup>2</sup>	$10^{-6}$
$R_{\theta}$ ( $^0$ ) <sup>2</sup>	$(0.1)^2$	$\theta_0$ ( $^0$ )	(0.1)	$P_{\theta}$ ( $^0$ ) <sup>2</sup>	$(10)^2$
$R_{\dot{\theta}}$ ( $^0/s$ ) <sup>2</sup>	$(0.01)^2$	$\dot{\theta}_0$ ( $^0/s$ )	(0.01)	$Q_{\dot{q}}$ ( $^0/s$ ) <sup>2</sup>	$10^{-8}$
$Q_{\theta}$ ( $^0$ ) <sup>2</sup>	$10^{-6}$	$Q_q$ ( $^0$ ) <sup>2</sup>	$10^{-8}$	$P_{q,\dot{q}}$ ( $^0, ^0/s$ ) <sup>2</sup>	$(10)^2$

### 4. 1. Nominal Case

Figure 2 shows the actual and standard deviations for the angular position, elastic displacement, angular velocity, and rate of elastic displacement, in degrees and degrees/s respectively. Errors were calculated according to Eqs (24)-(25). From Figure 2, one notices that most of the actual errors are within one standard deviation of Eq. (24). Convergence was attained quickly (less than 20s) for all but the angular position, although it was within 0.05° from then on.

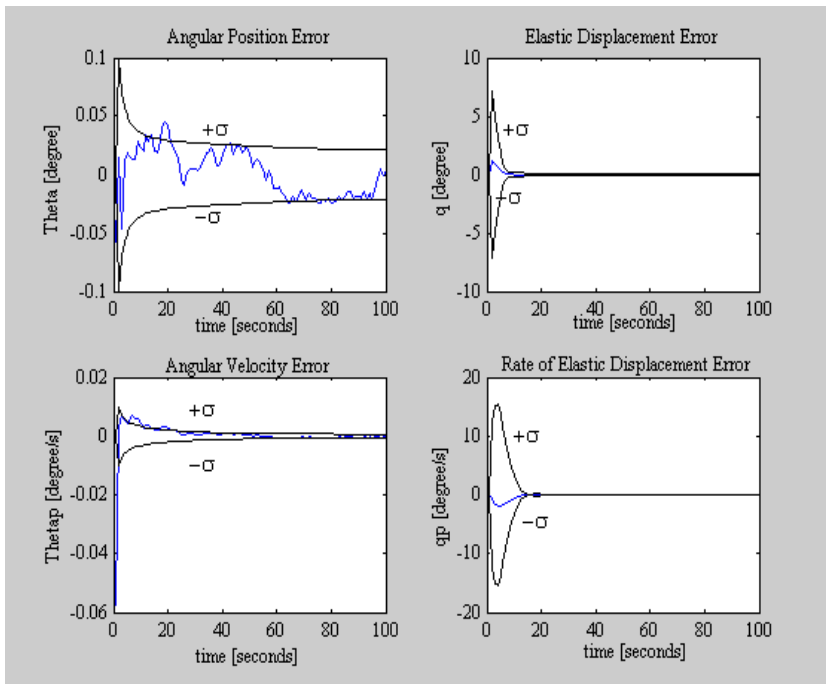


Figure 2. Angular error, Elastic displacement error, Angular velocity error, and rate of elastic displacement error.

Figure 3 shows the behavior of the measurement residuals on  $\theta$  and  $\dot{\theta}$  for the nominal case. In this case the residuals are in good shape with one standard deviation around  $0.1^\circ$  and  $0.01^\circ/\text{s}$ , respectively.

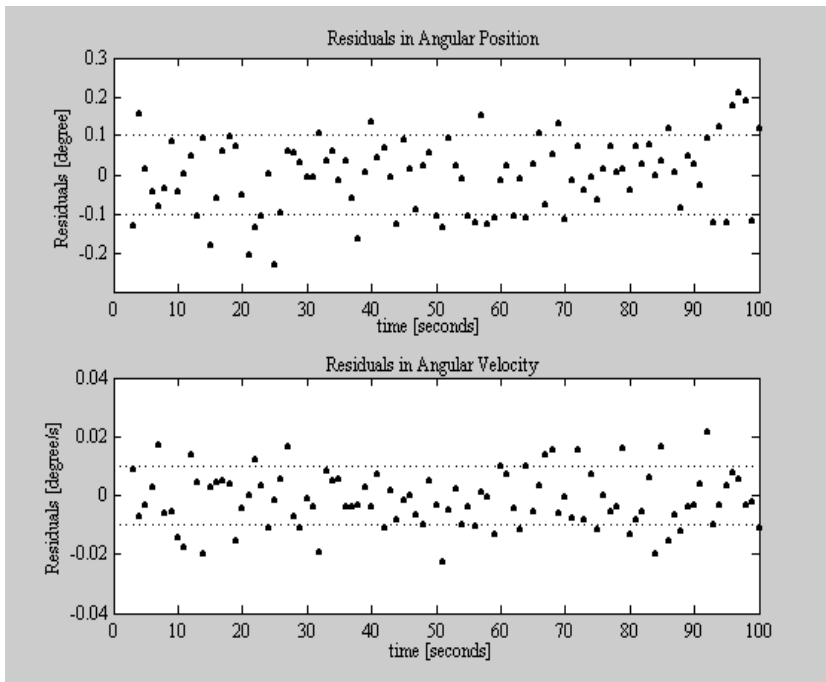


Figure 3. Residuals in angular position, and Residuals in angular velocity, nominal case.

#### 4. 2. Over-accurate measurements

In is case measurements are simulated with one order better accuracy. The aim is to verify if there is some relevant gain of accuracy in the identification filter when more accurate sensors are used. It can be observed in Figure 4 an apparent improvement in the residuals profile, one order better than the nominal case of Figure 3. This suggests better

state estimates with respect to the nominal case. For this case the angular position and velocity measurements were corrupted with random gaussian noise of  $0.01^\circ$  e  $0.001^\circ/s$ , respectively.

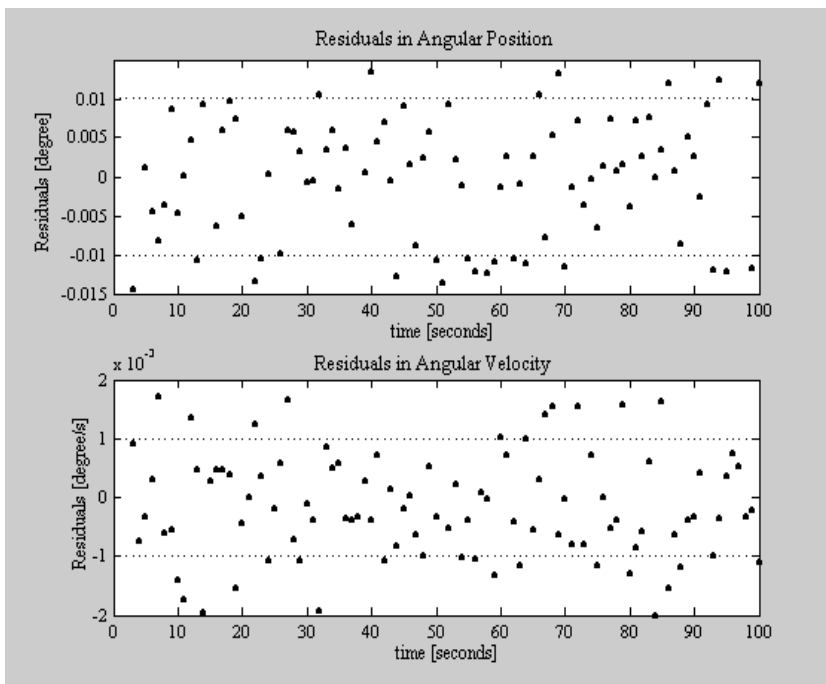


Figure 4. Residuals in angular position and Residuals in angular velocity, over accurate measurements case

### 4.3. Under accurate measurements

In the same way, one investigated the effects of less accurate (than nominal) measurements, with the aim of verifying if the accuracy is degraded up to the extent the filter does not estimate the states correctly. From Figure 5 it can be seen the influence of increasing the measurement errors in the behavior of the estimation scheme. From the simulations it can be seen that even losing sensors accuracy the filter shape did not degrade when compared to the nominal case, in terms of convergence. The measurement errors in this case were random gaussian with  $1^\circ$  and  $0.1^\circ/s$  of standard deviation, respectively. The behavior of the residuals in this under accurate measurements case is shown in Figure 5. Consistently the residuals RMS also increased one order of magnitude with respect to the nominal case. Moreover, the states were estimates without sign of divergence of the Kalman filter.

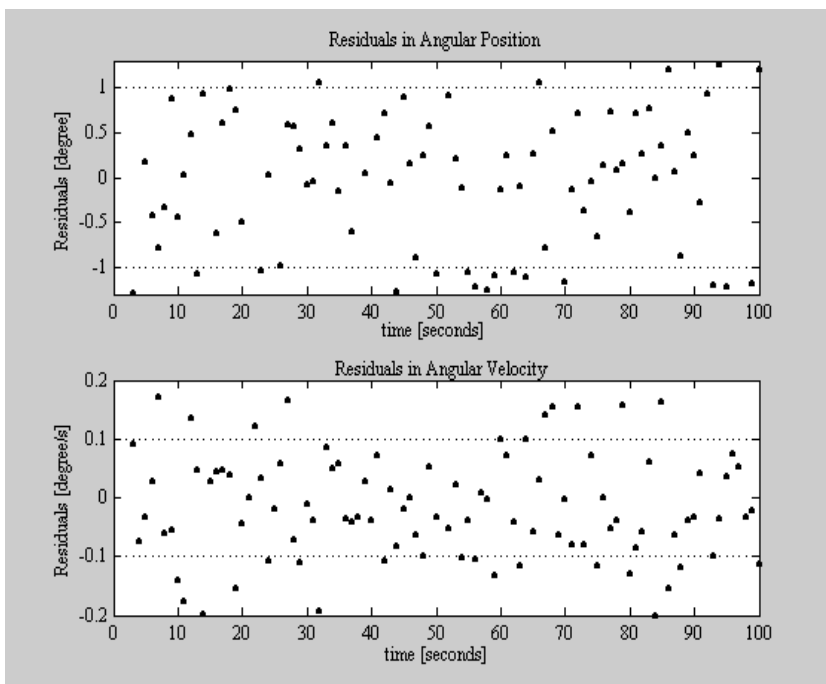


Figure 5. Residuals in angular position and Residuals in angular velocity, case of under accurate measurements

Table 2 lists the mean and the standard deviation of the states corresponding to the rigid body and the flexible part of the satellite. Through the table it can be observed that for the three cases, namely nominal, over-accurate, and under-accurate measurements, the state components regarding the flexible body,  $q$  (elastic displacement) and  $\dot{q}$ , did not suffer any meaningful change in the mean and in the standard deviation error. Nevertheless, the state components of the rigid body,  $\theta$  (angular position) and  $\dot{\theta}$  (angular velocity), suffered as expected with the variation of the noise in the measurement. In relation to the nominal case, all the cases tested converged to the expected level of errors, showing the robustness of the filter under several levels of measurement accuracy.

Table 2. Mean and standard deviation of state errors

	Nominal	Over accurate	Under accurate
$\theta$ ( $^{\circ}$ )	$(10^{-3}) \pm (2 \times 10^{-1})$	$(-3.6 \times 10^{-4}) \pm (6 \times 10^{-2})$	$(1.6 \times 10^{-2}) \pm (1 \times 10^0)$
$q$ ( $^{\circ}$ )	$(3 \times 10^{-2}) \pm (1.6 \times 10^{-1})$	$(3 \times 10^{-2}) \pm (1.6 \times 10^{-1})$	$(3 \times 10^{-2}) \pm (1.6 \times 10^{-1})$
$\dot{\theta}$ ( $^{\circ}/s$ )	$(2.7 \times 10^{-4}) \pm (6 \times 10^{-2})$	$(-5 \times 10^{-3}) \pm (6 \times 10^{-3})$	$(7 \times 10^{-2}) \pm (1.9 \times 10^{-1})$
$\dot{q}$ ( $^{\circ}/s$ )	$(-1.23 \times 10^{-1}) \pm (4 \times 10^{-1})$	$(-1.2 \times 10^{-1}) \pm (4 \times 10^{-1})$	$(-1.2 \times 10^{-1}) \pm (4 \times 10^{-1})$

## 5. Conclusion

In this work a satellite composed of a central rigid body and two flexible appendages was mathematically modeled to be used in an identification methodology based on Kalman filter. A Lagrangian formulation was used to derive the equations of motion of the satellite. A discretization of the elastic motion was performed by the assumed modes method. In the sequel the Kalman filter methodology using the Matlab package was implemented in order to identify the satellite rigid and flexible mode (states) composed of the rigid and elastic displacement and their variation in time. Throughout several simulations it was possible to investigate the behavior of the state estimation errors for three distinct cases. In the first one, called nominal case, typical data were considered as the initial conditions of the filter. In this case, it was verified that the satellite position and angular velocity errors estimates are within the errors allowed by the filter, being observed a great time for the convergence of the filter in the angular position component. For the elastic displacement and rate the convergence has occur in less than 20 seconds. Afterwards, two simulations considering non-typical conditions, that is, over accurate measurements and under accurate measurements has been investigated. For the over accurate case (as expected) it was detected a remarkable improvement in the real and estimated states with respect to the nominal case, that fact is due to the more accurate sensors. In the under-accurate case, it was detected that even with less accuracy of the sensors, the estimated state errors were not so degraded with respect to the nominal case, keeping the filter convergence in acceptable level. Having in mind the complexity of putting a sensors on the elastic parts of the satellite, the application of the Kalman filter methodology has been showed a good approach to identify indirectly the flexible parameters of a rigid-flexible satellite. That approach becomes more promising when it is necessary to feedback the elastic measurement into the control system in order to assure better pointing conditions and/or better system performance. The Kalman filter has also shown to be a robust methodology since in the under-accurate case tested, it has maintain a good performance. Therefore, being an important tool in the parameters identification phase of similar control systems.

## 6. References

- Chiaradia, A. P. M., Determinação e Manobras Autônomas de Órbitas de Satélites Artificiais em Tempo Real usando Medidas GPS de uma Frequência. São José dos Campos. Tese de Doutorado em Engenharia e Tecnologia Espacial- Instituto Nacional de Pesquisas Espaciais, 2002. INPE – 8755-TDI/198.
- Gelb, A.; Kasper Jr., J.F.; Nash Jr., R.A.; Price, C.F; Sutherland Jr., A.A. Applied Optimal Estimation. Inglaterra: The M.I.T Press, 1974. 374p.
- Guera, R.; Sandri, S. A.; Souza, M.L. O. “Dynamics and Design of Autonomous Attitude Control of a Satellite Using Fuzzy Logic”. Anais do COBEM’97, COB 1338, Bauru (SP), Dezembro, 1997.
- Silva, A.R.; Souza, L.C.G. “Control System Flexible Satellite Interaction During Orbit Transfer Maneuver”. Published by American Astronautical Society (AAS) in Advances in the Astronautical Sciences, Vol. 100 Part I, pp. 541-550, paper AAS 98-343, Ed. Thomas H. Stengle, USA, 1998. ISBN 0-87703-453-2
- Silva, A R., Schäfer, B., Souza, L.C.G., “Identification and Sensor Failure Detection Algorithms Applied to Space Robotic Joint”. XI Colóquio Brasileiro de Dinâmica Orbital, Viçosa-MG, Brasil, 04 a 08 de novembro de 2002.
- Souza, L.C.G.; Silva, S. A., “Vibration Control of a Rigid-Flexible Satellite During Attitude Maneuver”. Publicação da ASME do 17<sup>th</sup> Biennial Conference on Mechanical Vibration and Noise, 12-16, September, Las Vegas – Nevada, USA, 1999.
- Trigolo, A. Estudo do Desempenho do Sistema de Controle de Atitude de um Satélite Rígido-Flexível. São José dos Campos. Dissertação Mestrado em Engenharia e Tecnologia Espacial- Instituto Nacional de Pesquisas Espaciais, 2002.